Fourier Transform Infrared Study on the Encapsulation of CO in Zeolite Y under the Moderate Temperature and Pressure Conditions

B. S. Shete, V. S. Kamble, and N. M. Gupta*

Chemistry Division, Bhabha Atomic Research Centre, Trombay, Mumbai 400 085, India

V. B. Kartha

Centre for Laser Spectroscopy, Manipal Academy of Higher Education, Manipal 576 119, India

Received: February 17, 1998; In Final Form: May 4, 1998

Six distinct C−O stretch vibrational bands of varying intensity and with maxima at 2120, 2136, 2150, 2170, 2182, and 2195 cm^{-1} were observed during the room-temperature adsorption of CO over NaY zeolite. This was accompanied by the appearance of a prominent band at 2356 cm^{-1} along with the sidebands at 2336, 2342−2348, and 2364−2370 cm^{-1} in the ν_3 region of CO_2 vibrations. The intensity and the frequency of these bands showed monotonic changes on evacuation, temperature rise, and exchange of Na^+ ions with a proton or a group IIA cation and also on using the isotopically labeled CO. For instance, the adsorption of isotopic $^{13}C^{16}O$ and $^{12}C^{18}O$ gases gave rise to a uniform red shift in all the major ν(CO) bands, corresponding to a frequency ratio of $\nu(^{13}CO)/\nu(^{12}CO) \approx 0.978$ and $\nu(C^{18}O)/\nu(C^{16}O) \approx 0.976$. Similarly, all the asymmetric stretching bands of CO_2 showed a uniform isotopic shift corresponding to $\nu(^{13}C)/\nu(^{12}C) \approx 0.971$. Furthermore, the intensity of most of the above-mentioned bands in ν(CO) and $\nu_3(CO_2)$ regions exhibited an exponential type growth behavior with increasing adsorbate pressure, though the extent of this growth was different for individual vibrations. No significant change was, however, observed in the frequency and the intensity of the hydroxyl region bands on adsorption of CO under experimental conditions of this study. Arguments are presented to show that the observations of this study are not in harmony with the reported modes of direct CO adsorption at the specific zeolitic sites such as the charge-balancing cations, Al^{3+} sites, or the Bronsted acid sites. Instead, the formation of the weakly held $(CO)_n$ and $(CO_2)_n$ molecular clusters occluded in the zeolitic cavities and stabilized under the cation field is in conformity with the data of this study.

Introduction

Small molecules, such as CO, CO_2, CH_4, C_2H_4, and C_6H_6, are widely employed as probes in order to investigate the distribution of cations in various zeolites and also to delineate the role played by cations, acid sites, and individual zeolitic cavities in the host−guest interaction process in these materials. Being a polar molecule, carbon monoxide has been extensively used to demonstrate that the charge-balancing cations, silanols (both external and internal), and the Lewis acid centers (Al^{3+} ions in extraframework and framework positions) in zeolites may independently serve as CO binding sites. The nature and the strength of this bonding is found to depend on various factors, such as the composition of zeolite and the temperature and pressure of CO adsorption.[1−13] For instance, Zecchina et al. have investigated CO adsorption over Y, X, and ZSM-5 zeolites,[6] and the vibrational bands observed in the range 2100−2300 cm^{-1} have been attributed to the carbon monoxide molecules bonded at different zeolitic sites, as is described later in detail. Most of these studies were, however, performed under the low-temperature, low-pressure conditions, and not much work has been devoted so far to the situations likely to occur under the actual catalytic reaction conditions. In a previous communication from this laboratory,[14] we used infrared specroscopy to demonstrate that the room-temperature adsorption of carbon monoxide on X zeolites gave rise to the formation of $(CO)_n$ molecular clusters entrapped in the supercages. The charge-balancing cations were shown to have considerable influence on the nature of these clusters. We have also reported the thermal desorption spectroscopy results to reveal the existence of multiple CO binding states in zeolite X which were found to be modified by the charge-balancing cations.[15,16] In continuation, we now report the results of our FTIR spectroscopic study on adsorption of CO over zeolite Y at temperatures in the range 300−470 K and at pressures of 10−500 Torr (1 Torr = 133.3 Pa). The effect of cation exchange on CO binding states has been evaluated. The isotopically labeled ^{13}CO and $C^{18}O$ gases were also used in this study to monitor the shift in different vibrational bands.

Experimental Section

Samples. NaY zeolite sample (Si/Al ratio ∼ 2.7, surface area ∼550 $m^2\ g^{-1}$) was supplied by the Research and Consultancy Directorate of the Associated Cement Companies Ltd., Thane, India. The template free samples were used in this study after proper washing and drying. The test of chemical purity of zeolite by spectrographic analysis confirmed that, besides the presence of about 800 ppm of Fe and 10−50 ppm of Mg, Ti, and Mn, no other metal impurities were present beyond their detection limits. The CaY sample was prepared by repeated contacts of NaY zeolite with 10% calcium nitrate solution at a temperature of ∼335 K and at a pH of about 6. After a thorough

* To whom correspondence should be addresssed. Fax 91-22-5560750, E-mail nmgupta@magnum.barct1.ernet.in.

S1089-5647(98)01178-X CCC: $15.00
Published on Web 06/29/1998

washing and drying at 400 K the sample was calcinated at 720 K for 8 h. The HY sample was similarly prepared using an ammonium nitrate solution for exchange. The extent of exchange in both the HY and CaY samples was in the range 75−80%. NaY and the cation-exchanged samples used in this study were highly crystalline, and their XRD patterns matched with the data reported for single-phase Y zeolite.[17]

IR Spectroscopy. The self-supporting sample wafers of 25 mm diameter and weighing about 80 mg were mounted in a high-temperature, high-pressure IR cell fitted with water-cooled CaF_2 windows, details of which are given elsewhere.[14,18] A Mattson model Cygnus 100 FTIR equipped with a DTGS detector was used in this study. A sample was heated in situ for 25−30 h at a temperature of 600−625 K and under a vacuum of $\sim 1 \times 10^{-4}$ Torr before recording a background spectrum. CO at varying pressures was then introduced in the cell while maintaining the sample wafer at a desired temperature in the range 300−475 K. Normally 300 scans were added for each spectrum recorded at a resolution of 4 cm^{-1}, and a difference spectrum was then plotted as per the standard procedure. To compensate for the vibrational bands due to gaseous CO present in the cell, the CO gas spectra were recorded at different pressures without a sample wafer in the cell. The spectra due to adsorbed species were then plotted by subtracting the CO gas spectrum of appropriate intensity from the IR spectrum of the sample. The numbers given in parentheses in different figures show the absorbance value for individual vibrational bands which is taken as a measure of their relative intensities. The frequency values of individual vibrational bands were generally reproducible within $\pm 1-2$ cm^{-1} in the experiments repeated from time to time.

To take advantage of better resolution of the vibrational bands in the O−D stretching region as compared to the ν(OH) region, the deuteroxylated samples were used in this study to monitor the effect of CO adsorption on the hydroxyl region vibrations of zeolites, and the samples for this purpose were prepared by the repeated in situ contacts of NaY and CaY zeolite wafers in IR cell to deuterium gas at 600 K.

The overlapping spectral bands were separated using a deconvolution program in the computer software of FTIR in order to determine the number and the position of the individual peaks. Following deconvolution parameters were employed for this purpose: full width at half-maximum (w) = 12−14, enhancement factor (k) = 1.3, fraction Lorentzian (f) = 0.3, and the apodization or smoothing function (a) = 3. The relative integral areas under different IR bands were estimated by resolution of the overlapping bands using the origin 4.1 package of Microsoft Windows 95. A choice of the multiple Gaussian peaks gave an excellent fit for all the spectra.

Carbon monoxide (99.9% purity, from Airco, USA) was purified before use by enclosing in a solid carbon dioxide trap (195 K) in order to remove the traces of the metal carbonyl and moisture impurities. ^{13}C-labeled (∼60%) CO (Prochem Ltd, UK) and $C^{18}O$ (99.8 atom % ^{18}O and 0.003% ^{17}O) from Johnson Matthey (USA) were used for the isotopic studies.

Results

CO Adsorption over NaY Zeolite. A NaY zeolite wafer pretreated under vacuum at 600 K and then exposed at ambient temperature to 100 Torr of CO gave rise to an IR spectrum shown in Figure 1 a. The IR bands in the 2000−2250 cm^{-1} region superimposed over PR bands of gaseous carbon monoxide and the bands in the 2250−2400 cm^{-1} region due to ν_3 vibration of carbon dioxide may be noticed in this figure. No

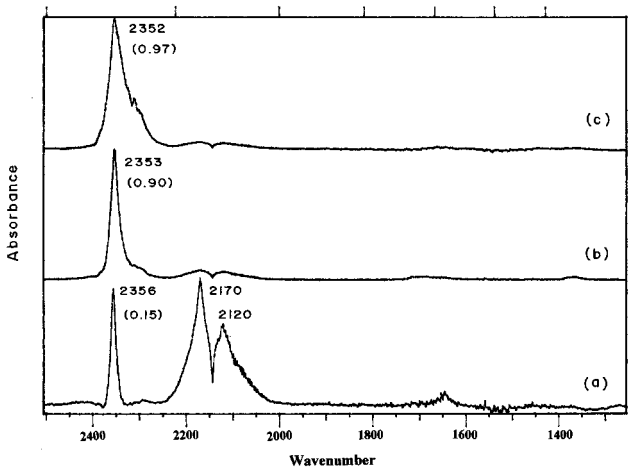

Figure 1. IR spectra of NaY zeolite exposed to 100 Torr of CO at (a) 300 K, (b) 370 K, and (c) 470 K.

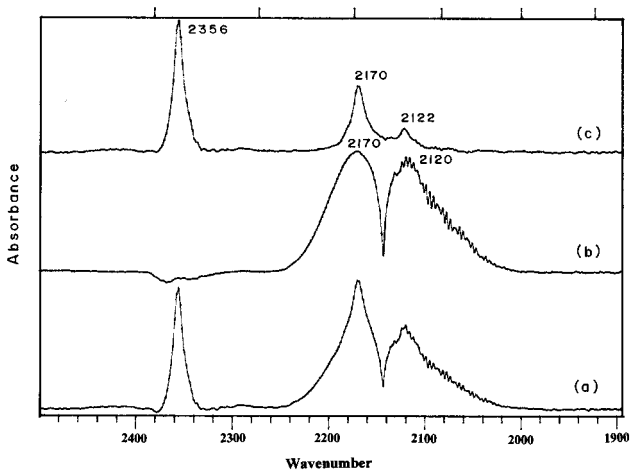

Figure 2. IR spectra of (a) NaY zeolite exposed to 100 Torr of CO at 300 K and (b) PR branches for 100 Torr of CO gas at 4 cm^{-1} resolution recorded without zeolite wafer. Curve c shows a difference spectrum (a) − (b).

bands in the 1200−2000 cm^{-1} region are seen in Figure 1, in contrast to the case of NaX zeolite[14] where two pairs of prominent bands, with maxima at 1711 and 1365 cm^{-1} for one pair and at 1488 and 1431 cm^{-1} for the other, were observed. The intensity and the width of the CO_2 stretch band increased on prolonged exposure of zeolite wafer to CO, and a saturation stage was reached in around 30−45 min. All the data included in this paper were therefore recorded after 30 min contact of a zeolite wafer with CO gas.

The rise in sample temperature resulted in the diminished intensity of C−O stretch region bands while the intensity of the $\nu_3(CO_2)$ bands was found to increase progressively, as shown by spectra b and c of Figure 1. Thus, the absorbance of the $\nu_3(CO_2)$ band increased by a factor of about 6 for the rise in sample temperature from 300 to 370 K [Figure 1b]. Rise in sample temperature to 470 K led to a broadening of the CO_2 vibrational band and to a further increase in its intensity [Figure 1c].

Spectra a and b in Figure 2 show the limited range vibrational bands of a NaY wafer exposed to 100 Torr of CO and of 100 Torr of CO gas in an IR cell (without sample), respectively. Spectrum c was obtained by subtracting spectrum b from Figure 2a so as to compensate for the unadsorbed CO in the cell. Almost complete absence of PR rotational bands confirms that the IR bands in Figure 2c are exclusively due to CO adsorbed

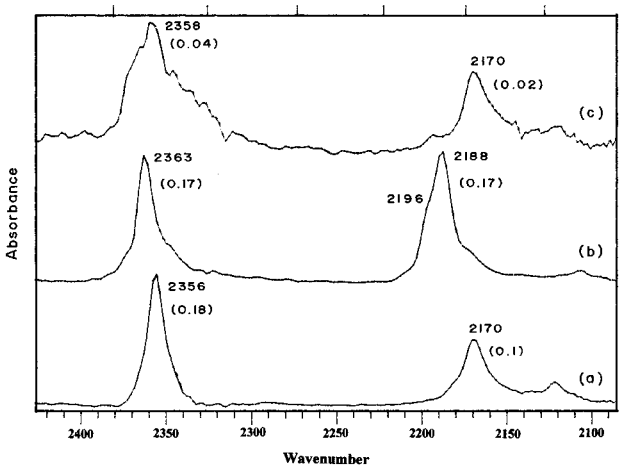

Figure 3. Change in frequency and intensity of ν(CO) IR bands when 100 Torr of CO was dosed over (a) NaY, (b) CaY, and (c) HY zeolite.

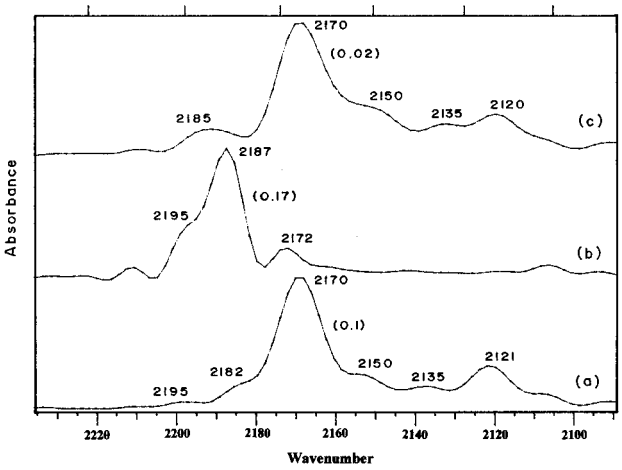

Figure 4. Deconvolution of ν(CO) IR bands developed on 100 Torr of CO exposure over (a) NaY, (b) CaY, and (c) HY zeolite.

in the zeolite sample. The data reported henceforth in this paper, except in Figure 16, refer to such difference spectra. The difference spectra for CO adsorption on NaY at sample temperatures of 370 and 470 K [Figure 1 b,c] showed that practically no CO was adsorbed in zeolites at the temperatures above 370 K.

Effect of Cation Exchange. Figure 3 presents the typical data on the effect of substituting Na^+ with Ca^{2+} and H^+ ions. The absorbance values given in these spectra show that, as compared to NaY, the amount of CO adsorbed in CaY increased by a factor of ~1.7 while the intensity of the $\nu_3(CO_2)$ band was almost the same [Figure 3b]. On the contrary, the intensity of both the CO and CO_2 stretching bands was around one-fourth in the case of HY as compared to NaY [Figure 3c]. Also, two weak bands at 1425 and 1440 cm^{-1} were observed for the CO adsorption over CaY in contrast to Na^+ (data not shown). More details on the effect of cation exchange on the CO adsorption behavior of zeolites are given elsewhere.[19] A clear picture of the position and the relative intensity of the different overlapping bands emerges on the deconvolution and the computer resolution of different spectra, as shown below.

Resolution of Vibrational Bands. Spectra a−c in Figure 4 present the deconvolution of C−O stretching bands for NaY, CaY, and HY zeolites corresponding to spectra a−c in Figure 3. Figure 4a clearly reveals the presence of at least six distinct ν(CO) bands, namely at around 2121, 2135, 2150, 2170, 2182, and 2195 cm^{-1} during the adsorption of CO on NaY zeolites.

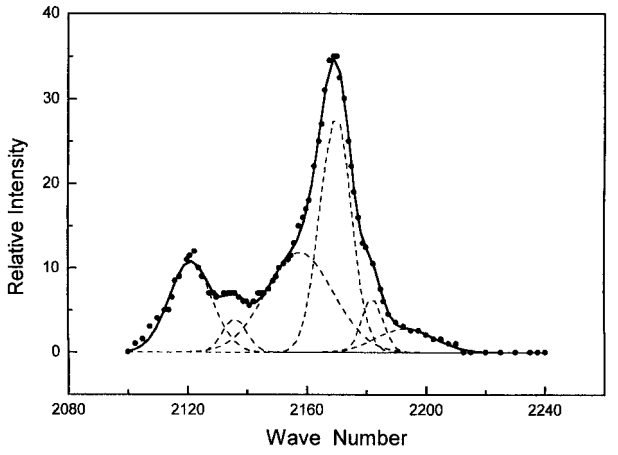

Figure 5. Computer resolution of the ν(CO) region overlapping IR bands formed on NaY zeolite after exposure to 100 Torr of CO at 300 K.The solid line is the sum total of the component bands.

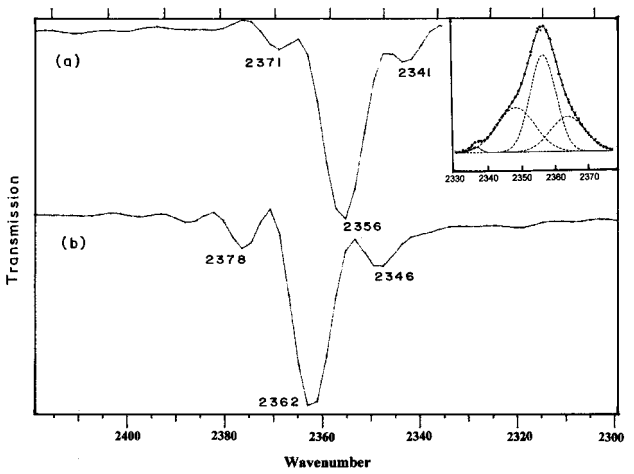

Figure 6. Deconvolution of the asymmetric stretch region bands of CO_2 developed over (a) NaY and (b) CaY zeolite after exposure to 100 Torr of CO at ambient temperature. Inset: computer resolution of the overlapping $\nu_3(CO_2)$ bands of NaY.

The existence of these distinct bands is confirmed again from their growth behavior as a function of increasing CO pressure, as described later in the text.

Exchange of Na^+ with Ca^{2+} cations resulted in the diminished intensity of the bands in the 2120−2150 cm^{-1} region [Figure 4b]. At the same time, the higher frequency bands at 2170, 2182, and 2195 cm^{-1} in Figure 4a appear to show a uniform blue shift of about 16 ± 2 cm^{-1}. Bands at frequencies similar to those in NaY [Figure 4a] were also observed for the CO adsorption on HY, even though the intensity of all the bands was uniformly smaller compared to that of NaY zeolite [Figure 4c], as is evident from the absorbance values given in this figure.

Figure 5 presents a computer band fitting of the C−O stretching bands appearing in Figure 3a. While the circles in this figure show the data points, the solid line envelope curve represents the sum of the component bands plotted in dotted lines. The formation of six distinct peaks in this region as a result of the room-temperature adsorption of CO on NaY is clearly indicated in this figure.

The IR bands in the ν_3 region of CO_2 stretch can similarly be resolved into at least four component bands with their frequency maxima at 2336, 2342, 2356, and 2370 cm^{-1}. Figure 6 presents a deconvolution of the bands in this region for the 100 Torr of CO adsorption at ambient temperature on NaY and CaY zeolites, corresponding to spectra a and b in Figure 3. A

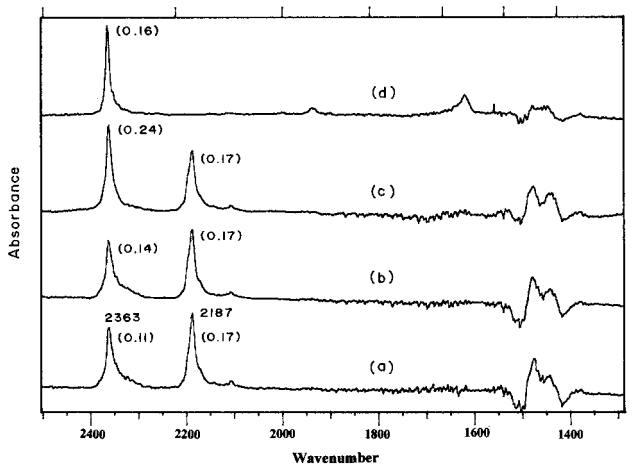

Figure 7. IR spectra of CaY zeolite outgassed at 570 K for (a) 3 h, (b) 8 h, and (c) 20 h prior to exposure to 100 Torr of CO at room temperature. Curve d was recorded after 15 min evacuation of sample c.

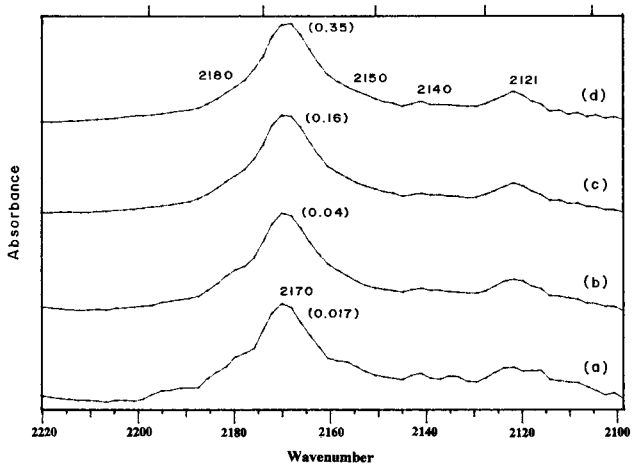

Figure 8. ν(CO) region IR bands developed over NaY zeolites after the ambient temperature exposure to CO at different pressures of (a) 20, (b) 50, (c) 200, and (d) 500 Torr.

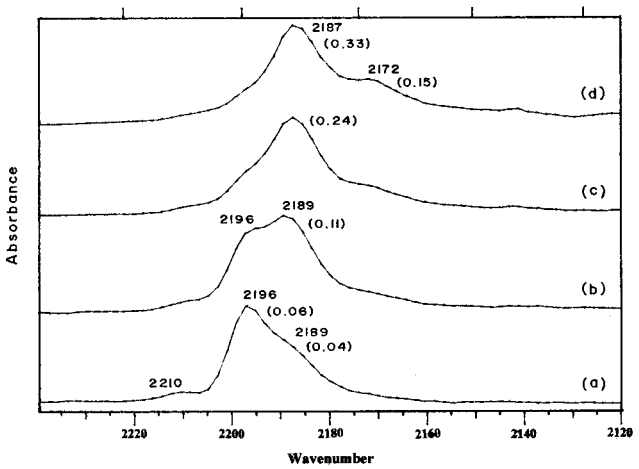

Figure 9. C−O stretch region IR bands developed over CaY zeolite after room-temperature exposure to CO at different pressures of (a) 10, (b) 50, (c) 200, and (d) 500 Torr.

computer band fitting of these bands in the typical case of NaY zeolite is shown in the inset of Figure 6, revealing again the presence of at least four distinct vibrational bands in this region with a marginal difference in their frequency compared to that given in Figure 6a. As in the case of ν(CO) bands [Figure 4b], all the bands in the ν_3 region of CO_2 stretch also showed a positive shift of about 6 cm^{-1} in the case of CO adsorption on CaY. No measurable frequency shift in these bands was, however, noticed in the experiments using HY zeolite [Figure 4c].

The intensity of both the ν(CO) and ν_3 region bands of CO_2 depended on various parameters, such as the pretreatment given to a sample, adsorption temperature, and adsorbate pressure, as is described below.

Effect of Pretreatment. Evacuation of the sample for longer durations at 600 K prior to CO exposure resulted in more intense $\nu_3(CO_2)$ bands while the intensity of the ν(CO) region bands remained almost unchanged. Typical data on the effect of sample pretreatment on vibrational bands formed on CaY zeolite after 100 Torr of CO adsorption at room temperature are included in Figure 7. A comparison of spectra given in Figure 7a,c shows that the intensity ratio i.e., $I(CO_2)/I(CO)$, as evaluated from the absorbance value, was ∼1.4 for a sample pretreated for 24 h [Figure 7c], compared to a value of around 0.75 after 3 h of evacuation. A similar trend was noticed for the NaY zeolite.

Effect of Evacuation. Evacuation of the IR cell after CO exposure at 300 K resulted in the quick removal of all the C−O stretch region IR bands, in both the NaY and the cation-exchanged samples. The CO_2 stretch bands, however, showed a higher stability in the case of the CaY sample. Thus, while these bands were removed completely in NaY within 3−4 min of pumping at room temperature, they could be observed even after 30 min of postexposure evacuation of CaY zeolite, though with a reduced intensity. Spectrum d in Figure 7 shows the vibrational bands recorded after 15 min evacuation of a CaY sample exposed to 100 Torr of CO (Figure 7c).

Effect of CO Pressure. *C−O Stretch Bands*. Figures 8 and 9 present the overlay spectra of C−O stretch region bands developed on NaY and CaY zeolites as a function of CO pressure in an IR cell. These data show that the frequency of different bands remained almost unchanged on increasing CO gas pressure from 10 to 500 Torr in the case of both zeolite samples, even though their intensities showed significant changes. The pressure effect on the relative areas of some of the ν(CO) region bands formed during adsorption of CO over NaY and CaY zeolites is presented in Figure 10. The data in this figure show that, except for a band at 2196 cm^{-1} in the case of the CaY sample (Figure 10f), all other bands showed a near linear growth in the initial stages, their intensities changing asymptotically at higher pressures.

CO_2 Stretch Region Bands. As in the case of ν(CO) bands, the intensity of all the vibrational bands in the asymmetric CO_2 stretch (ν_3) region also increased progressively with the rise in CO gas pressure for both the samples used in this study. Figure 11 presents the typical spectra in ν_3 region of CO_2 for CO adsorption over NaY zeolite at different pressures along with their corresponding absorbance data. Again, as in the case of ν(CO) bands, the extent of growth in the individual $\nu_3(CO_2)$ region bands was also different. Thus, while the 2356 and 2342 cm^{-1} bands showed larger increase in their intensity, the intensity of the other two bands changed only marginally with the rise of adsorbate pressure. A small but reproducible red shift ($\Delta\nu \approx -2$ cm^{-1}) in the frequency of this band may also be noticed (Figure 11).

The fractional area covered under the individual vibrational bands (area under a band divided by total area under different ν(CO) or $\nu_3(CO_2)$ region bands at a particular pressure),

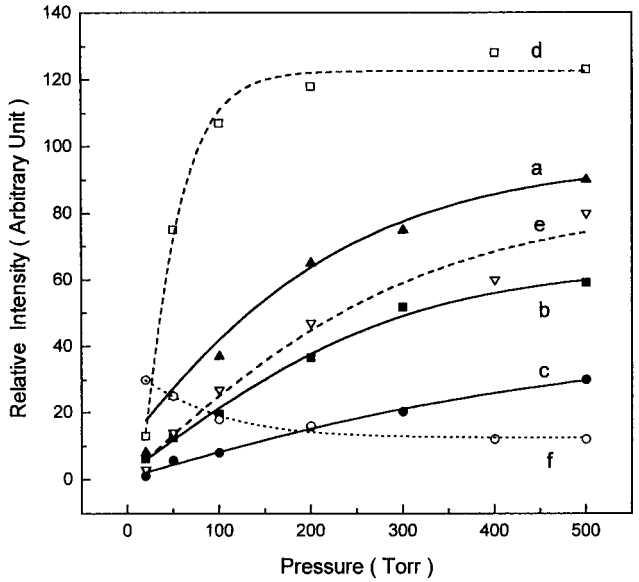

Figure 10. Pressure dependence of the intensity of some representative ν(CO) bands formed on room-temperature exposure of carbon monoxide over NaY (a−c) and CaY (d−f) zeolites: (a) 2170$^-$, (b) 2120$^-$, (c) 2150$^-$, (d) 2187$^-$, (e) 2172$^-$, and (f) 2196 cm^{-1}.

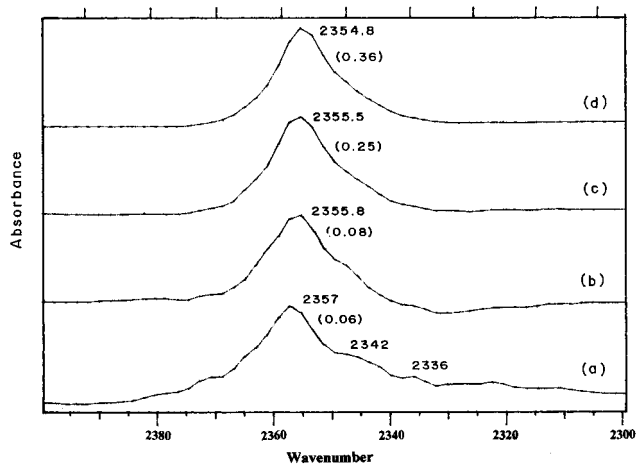

Figure 11. The ν_3 vibrations of CO_2 developed over CaY zeolite on ambient temperature exposure to CO at different pressures of (a) 20, (b) 50, (c) 200, and (d) 500 Torr.

however, showed a different trend. Thus, while some of the bands showed a large increase in the relitive intensity, the area covered by some other bands was found to reduce considerably. On the other hand, the intensity of some of the vibrational bands remained almost unchanged. Typical data in the case of a CaY zeolite are presented in Figure 12 for the ν(CO) region bands.

Adsorption of Labeled CO. Irrespective of the nature of a charge-balancing cation, all the bands in the C−O stretch region showed a negative shift of ∼48 cm^{-1} on adsorption of ^{13}CO corresponding to an isotopic shift of $\nu(^{13}CO)/\nu(^{12}CO) \approx 0.978$. Similarly, these bands showed a uniform shift of $\Delta\nu = -50 \pm 1$ cm^{-1} on adsorption of $^{12}C^{18}O$. Spectra a−c in Figure 13 show the typical C−O stretch vibrational bands of CaY zeolite exposed to $^{12}C^{16}O$ (20 Torr), $^{12}C^{16}O + {}^{13}C^{16}O$ (2:3, 50 Torr), and $^{12}C^{18}O$ (20 Torr), respectively. These spectra are presented in deconvoluted form for better discrimination of the component bands. The position of different C−O stretching bands and their isotopic shifts during the adsorption of labeled CO are presented in Table 1, for both the NaY and the CaY zeolite samples.

A similar trend was seen in the case of the isotopic shifts in ν_3 vibrational bands of CO_2 also, as is shown in the IR spectra

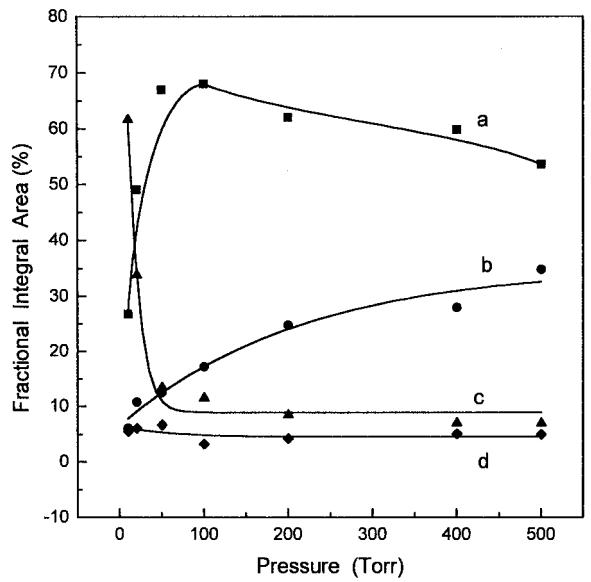

Figure 12. Fractional integral area of some representative ν(CO) bands developed on CaY zeolite after room-temperature adsorption of CO at different pressures.

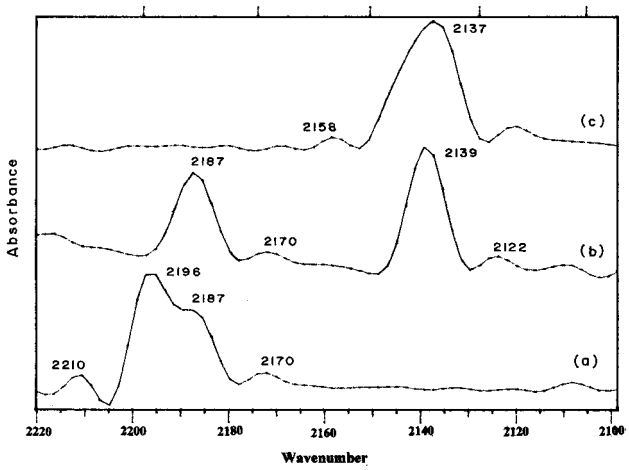

Figure 13. Deconvoluted spectra of CaY in the ν(CO) region after exposure to (a) $^{12}C^{16}O$ (20 Torr), (b) $^{12}C^{16}O + {}^{13}C^{16}O$ (50 Torr), and (c) $^{12}C^{18}O$ (20 Torr).

of Figure 14. The corresponding frequency data are given in Table 2. A comparison of spectra a and b in Figure 14 reveals that all the component bands in this region show a red shift of 67.5 ± 0.5 cm^{-1} in the experiment for ^{13}CO adsorption. On the other hand, the adsorption of $^{12}C^{18}O$ resulted in the shift of 2376, 2363, and 2351 cm^{-1} bands to the new frequencies of 2342, 2328, and 2315 cm^{-1}, amounting to a $\Delta\nu$ value of 35 ± 1 cm^{-1} (Figure 14c).

Effect of CO Adsorption on Hydroxyl Bands. Figure 15 presents the vibrational bands of deuteroxylated NaY and CaY zeolites before and after exposure to 100 Torr of CO at ambient temperature. A spectrum due to the undeuteroxylated zeolite sample has been subtracted from these spectra to compensate for the background. The sodium form of Y zeolite showed no strong OH/OD bands, and only a single weak band at around 2729 cm^{-1} was observed in this case (Figure 15a). This is in agreement with the fact that the dehydrated form of NaY zeolite does not exhibit a protonic character.[20] On the other hand, the CaY zeolite showed five distinct bands at 2759, 2719, 2687, 2646, and 2600 cm^{-1} (Figure 15b). The frequency and the shape of the O−D stretch bands remained unaffected when both the NaY and CaY zeolites were exposed to CO under the

TABLE 1: Isotopic Shift of Some Prominent C−O Stretching Hands Arising after Room-Temperature Adsorption of $^{13}C^{16}O$ and $^{12}C^{18}O$ Gases over NaY and CaY Zeolites (Figure 14)

	NaY			CaY		
Sl no.	ν/cm^{-1} on $^{12}C^{16}O$ adsorption	$\nu^{13}C^{16}O/\nu^{12}C^{16}O$	$\nu^{12}C^{18}O/\nu^{12}C^{16}O$	ν/cm^{-1} on $^{12}C^{16}O$ adsorption	$\nu^{13}C^{16}O/\nu^{12}C^{16}O$	$\nu^{12}C^{18}O/\nu^{12}C^{16}O$
1	2122	0.9778	0.9764	2170	0.9778	0.9765
2	2157	0.9777	0.9758	2187	0.9780	0.9771
3	2169.7	0.9777	0.9761	2196	0.9781	0.9767
4	2182	0.9771	0.9761	2207/2210	0.9773	0.9764

TABLE 2: Isotopic Shifts of Some Prominent ν_3 Region Bands of CO_2 Arising after Room-Temperature Adsorption of $^{13}C^{16}O$ and $^{12}C^{18}O$ Gases over NaY and CaY Zeolite (Figure 15)

	CaY			NaY	
Sl no	ν/cm^{-1} on $^{12}C^{16}O$ adsorption	$\nu^{13}C^{16}O/\nu^{12}C^{16}O$	$\nu^{12}C^{18}O/\nu^{12}C^{16}O$	ν/cm^{-1} on $^{12}C^{16}O$ adsorption	$\nu^{13}C^{16}O/\nu^{12}C^{16}O$
1	2351	0.9710	0.9849	2342	0.9710
2	2363	0.9712	0.9852	2356	0.9719
3	2376	0.9718	0.9856	2371	0.9713

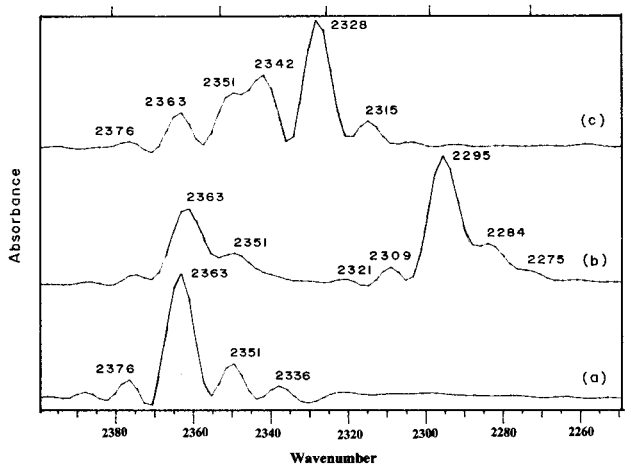

Figure 14. Deconvoluted spectra of CaY zeolite in the ν_3 region of CO_2 after exposure to (a) $^{12}C^{16}O$ (20 Torr), (b) $^{12}C^{16}O$ + $^{13}C^{16}O$(50 Torr), and (c) $^{12}C^{18}O$ (20 Torr).

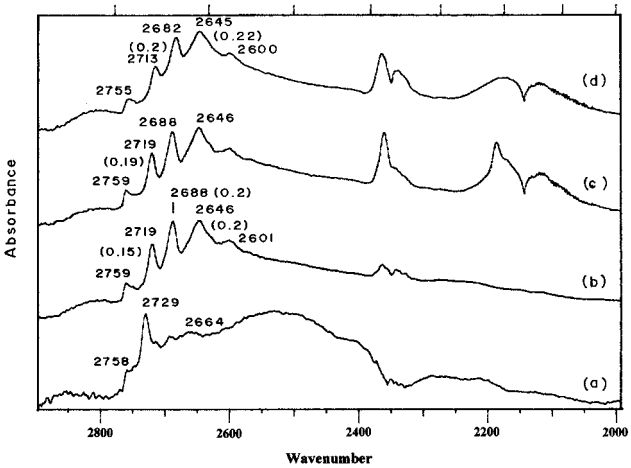

Figure 15. O−D region stretch bands of (a) NaY and (b) CaY zeolite after in situ deuteroxylation in deuterium atmosphere. Spectra c and d were recorded after dosing 100 Torr of CO over sample b at 300 and 570 K, respectively.

experimental conditions of this study. Also, the intensity of these bands was reduced only marginally during CO exposure at an elevated temperature of 470 K, the effect being negligible at lower temperatures. Spectra c and d in Figure 15 show these bands after 100 Torr of CO exposure over CaY zeolite at 300 and 470 K, respectively.

Adsorption of CO over γ-Alumina and Silica. Exposure of carbon monoxide over finely ground γ-alumina and silica gave rise to C−O stretching bands similar that of gas-phase CO (Figure 2b), and thus no CO was found to adsorb and similarly no CO_2 bands were developed on these samples under the experimental conditions of this study.

Discussion

The adsorption of CO on zeolites and on other metal oxides (MgO, γ-Al_2O_3, SiO_2, SiO_2−Al_2O_3, TiO_2, CeO_2, etc.) is found to give rise to carbonyl stretching bands at frequencies both lower and higher than that of gas-phase CO (∼2143 cm^{-1}).[21−24] The intensity and the position of these bands are shown to depend on various factors, such as the sample temperature, adsorbate pressure, and the nature of the substrate. These bands have been assigned to different modes of CO bonding. For example, the vibrational bands in the 2150−2220 cm^{-1} region on the surfaces of alumina and dehydroxylated zeolites are attributed to the dative σ-bonding of CO molecules with the framework Al^{3+} ions (Lewis acid sites), which are known to serve as electron acceptors.[8,21−24] The charge-balancing cations in the zeolites are similarly identified as the centers involved directly in CO bonding. In an early study, Angell and Schaffer[1] demonstrated that the adsorption of carbon monoxide on X and Y faujasites gave rise to two modes of adsorption; in the first type the carbon monoxide molecules are attached to the cations giving rise to an IR band at 2170 cm^{-1}, the frequency of which depended significantly on the nature of the charge-balancing cation. It was also demonstrated in this study that the frequency of CO adsorbed in faujasites increased linearly with the field strength induced in the zeolitic pores by divalent charge-balancing cations. Such a relationship has been corroborated in subsequent studies.[3] More recent studies on this subject have shown the development of various IR absorption bands in the 2000−2400 cm^{-1} region during the low-temperature adsorption of carbon monoxide on Y, X, and ZSM-5 type zeolites.[6−9] In these studies, a prominent absorption band in the 2160−2180 cm^{-1} range is ascribed to the stretching mode of the C−O bond in carbon monoxide molecules, polarized by Na^+ or H^+ ions inside the zeolite supercages of faujasites or the channels of ZSM-5 zeolites. Also, a weak band at 2115 cm^{-1} is assigned to CO molecules doubly coordinated to a cation and a Lewis acid center. A prominent band is also observed at 2138 cm^{-1} in these studies which has been identified with the liquidlike CO held inside the zeolitic cages. Transmission IR spectroscopy has also been employed to demonstrate the perturbing effects

of adsorbed CO molecules on the surface hydroxyl groups of silica.[11−13] This is attributed to the bonding of CO molecules on the hydrogen atom of acidic OH groups which is accompanied by a noticeable red shift of the O−H vibrational frequency and a blue shift in the frequency of the ν(CO) band. The CO stretch bands at 2158 and 2140 cm^{-1} have been attributed in these studies to the physical adsorption of CO on the Bronsted sites of SiO_2.[11−13] It may however be pointed out that most of the studies cited above pertain to CO adsorption at around liquid nitrogen temperature, and only scanty spectroscopic studies have been reported so far on the species formed over zeolite surface during the adsorption of CO at higher temperature and pressure conditions.

With this background we shall now attempt to discern the results of this study in light of the above-mentioned modes of direct CO bonding at different zeolitic sites.

The 2100−2200 cm^{-1} Region Bands. 1. All the bands observed in the C−O stretching region show a uniform isotopic shift (Figure 13, Table 1) on the adsorption of ^{13}CO and $C^{18}O$. These shifts ($^{13}C/^{12}C \sim 0.978$ and $^{18}O/^{16}O \sim 0.976$) are commensurate with the normal behavior expected in gas-phase molecules as per the simple isotopic shift rule, i.e., $\nu_1/\nu_2 = (\mu_2/\mu_1)^{1/2}$, and do not depend on the nature of the charge-balancing cations (Table 1). In the case of CO molecules bonded strongly to the distinct low-mass zeolitic sites, the bond strengths and the bond lengths will be different from one another, leading to different amounts of mixing with the vibrational modes of the rest of the system and will therefore result in varying amounts of isotopic shifts. We can thus infer that the ν(CO) IR bands observed in our study emanate from some loosely bonded CO species and not from the CO molecules bonded fairly strongly to different zeolitic sites.

2. The width at the half-maximum of all the component bands varied from 12 to 28 cm^{-1} [Figure 5] as compared to a width of $\sim$55 cm^{-1} for the P and R branches in the vibrational bands of gaseous CO at 100 Torr pressure (Figure 2b). Also, the rotationless structure of these bands (Figures 2c, 3, and 4) clearly indicates that they arise from the CO molecules entrapped under certain ovarian conditions and not from the free CO gas molecules.

3. Data in Figure 10 show that in the case of both the NaY and CaY zeolites the intensities of most of the ν(CO) bands showed a similar growth behavior with the increasing adsorbate pressure, even though the extent of this growth was different. Such a behavior is unlikely to occur if the CO molecules are bonded at the specific binding sites of zeolites existing in their limited number.

4. The vibrational bands in the O−D stretch region, appearing at frequencies of around 2759, 2719, 2687, 2646, and 2600 cm^{-1} (Figure 15b), correspond with the reported hydroxyl group bands of CaY zeolite and show an expected isotopic shift $\nu(OD)/\nu(OH) \approx 0.7375$.[25] The ν(OD) band at 2759 cm^{-1} corresponds with the ν(OH) band observed for CaY at 3740 cm^{-1}, which is generally assigned to the silanol OH groups terminating at the exterior faces of the zeolite crystallites.[20−25] The lower frequency bands have been identified with the structural hydroxyl groups attached to the different oxygen sites in zeolitic framework and giving rise to the Bronsted acidity or to the cation sites.[20] Since no frequency shift is noticed in the O−D region bands after CO adsorption on CaY and also as similar ν(CO) bands were observed for NaY zeolite having no acidic hydroxyl groups (Figures 3 and 15), it is apparent that the six ν(CO) bands (Figure 5) observed in our study cannot originate from the CO molecules bonded at different hydroxyl groups.

5. The possibility of the bonding of CO molecules at Al^{3+} sites (Lewis acid sites) may also be ruled out on the basis that the intensity of all the ν(CO) bands reduced drastically on exchanging Na^+ with protons (Figure 3c) when the number of the aluminum sites remained almost unchanged. This is also supported by the fact that in the independent experiments no CO was found to adsorb on alumina surface under the identical pretreatment and reaction conditions of this study. Furthermore, although the mass of an Al atom is quite different from the mass of a C atom, it is still sufficiently low, and therefore if CO is bound to Al, it will cause the mixing of C−O and Al−C vibrations and hence will give rise to different isotopic shifts as compared to that of gaseous CO. The data in Figure 13 are therefore unlikely to be expected for the CO molecules bonded at framework Al^{3+} sites.

6. The adsorption of CO at energetically heterogeneous cation sites is another possible origin of the ν(CO) region bands. For a Y zeolite, S_I sites located at the center of the hexagonal prisms and S_{II} sites located in the sodalite cages are known to be the most preferred sites for bivalent cations. However, these sites are known to be inaccessible to molecules such as CO or CO_2,[26,27] and only S'_I and S'_{II} type sites located in super cages are thus available for CO bonding. It is thus evident that the bonding at cation sites alone cannot give rise to a number of distinct bands observed in this study. Also, this concept does not explain why the intensity of the νCO bands increased considerably on exchanging with Ca^{2+} cation (Figure 3).

7. As will be discussed later, ^{18}O isotope studies show that the formation of CO_2 (Figures 1−3) results entirely from CO that gets attached to an oxygen, thus resulting in the abstraction of the bound oxygen and leading thereby to monoisotopically labeled CO_2. This indicates that the binding of CO to oxygen is very strong, and consequently the isotope shifts produced will vary from site to site, due to mixing of the $C^{18}O$ vibrations with $C^{16}O$ or other vibrations. All the C−O bands, on the other hand, showed a uniform diatomic type isotopic shift as mentioned already. This precludes any strong binding of the CO to light atoms.

On the basis of the points made above, we may thus conclude that the multiple C−O stretching bands observed in our study may have their origin in the modes other than the direct bonding of CO molecules at specific zeolitic sites. These bands showing identical isotope shifts for ^{13}C and ^{18}O substitution may rather be envisaged to arise from the species formed as a result of adsorbate − adsorbate interactions giving rise to the formation of molecular CO clusters, as described below.

Thus, the development of a number of C−O stretching bands can be understood if we consider the formation of molecular clusters of carbon monoxide (dimers, trimers, etc.), entrapped in the zeolitic cages and stabilized under the cationic field. The mutual interaction of the individual monomer components in these clusters will result in the multiple modes of vibrations and hence in the multiple IR absorption bands, as shown in Scheme 1 for the one form of a dimer.

A dimer of carbon monoxide may thus give rise to two vibrational bands of different intensities, the b_1 band being more intense in the infrared. Similar modes of vibrations and hence the multiple IR bands will originate from a trimer of CO (Scheme 2).

Being of C_{3v} symmetry, a trimer cluster of CO will also be expected to give rise to two vibrational bands in infrared, the

SCHEME 1: Two Possible Modes of a Dimer Cluster of CO Molecule

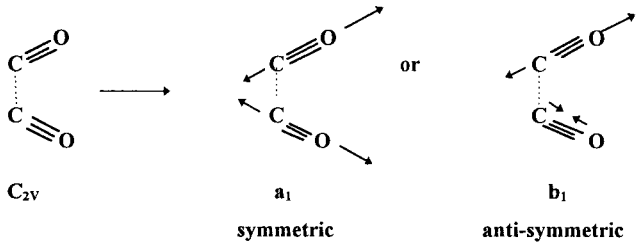

SCHEME 2: A Trimer of Carbon Monoxide

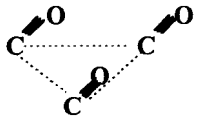

band due to a doubly degenerate (e) mode being more intense as compared to the other band due to a symmetric (a_1) mode of vibration. If the cluster size becomes too large, once again we may have a single band corresponding to a liquidlike system.

The pressure-dependent growth behavior of different IR bands in Figure 10 is commensurate with this viewpoint and can be well explained by the progressive increase in the concentration of such CO clusters. It is surmised that the saturation concentration of the individual type of clusters and their vibrational modes may depend on the zeolitic pore structure and the adsorbate pressure, thus giving rise to different slopes of growth curves in Figure 10.

Also, the growth behavior of ν(CO) bands, as seen in Figure 10, follows a trend similar to that reported by Rabo et al.[28] for the adsorption of CO in cation-exchanged Y zeolites where the pressure-dependent variation of the intensities of ν(CO) bands was found to follow a Langmuir type equation implying the adsorption on approximately equivalent, noninteracting or only weakly interacting sites. This again is in conformity with the conclusions reached in our study.

The data in Figure 12 may be interpreted to suggest that the relative concentration of some of these clusters (such as a dimer) reduces with increasing pressure (e.g., Figure 12c) while that of certain higher clusters (such as a trimer) shows an increase (Figure 12a). We may however mention that no attempt is made at present to establish a qualitative or a quantitative relationship between a specific cluster structure and the IR bands observed in our study. We are also not in a position now to comment on the largest possible cluster of CO that may form in the zeolitic pores. It is, however, pertinent to add here that the formation and the entrapment of large noble metal based carbonyl clusters (such as $Rh_6(CO)_{16}$ and $Ir_6(CO)_{15}$) in the zeolitic cages have been demonstrated widely.[29−32]

Spectra in Figure 3 clearly reveal a strong correlation between the charge-balancing cation and the relative intensity of the individual bands. A small shift in the frequency of these bands is also noticeable in the calcium-exchanged zeolite sample (Figure 3b). The intensity of various vibrational bands followed a general trend: CaY > NaY > HY. Also, the amount of CO held in HY zeolite (Figure 3c) is commensurate with the residual Na^+ concentration in this sample. This therefore indicates that the balancing cations are vital for the entrapment of CO. As the electrostatic potential (charge/radius) associated with H^+, Na^+, and Ca^{2+} has a value around 0.6, 1.0, and 1.9 V, respectively,[1] and this trend matches with the cation effect on the intensity of different bands in Figures 3 and 4, it is apparent that the electrostatic field of a charge-balancing cation plays an important role in the formation and the stabilization of the molecular clusters. The clusters such as mentioned above (Schemes 1 and 2) will be bound by the weak dipole−dipole type forces, which is in agreement with the quick removal of the ν(CO) bands on pumping and also their absence in the experiments performed at higher temperatures (Figure 1). The vibrations of the two or more CO molecules clustered together can only be perturbed slightly; each C−O group will show the original isotope shift, and thus the isotope shift due to coupling will be negligible. For instance in a mixed dimer, i.e., $O{\equiv}{}^{12}C\text{---}{}^{13}C{\equiv}O$, the ^{12}CO will show the unshifted band and the ^{13}CO will show the isotopically shifted band. This is in agreement with the data of Figure 13.

The 2330−2380 cm^{-1} Region Bands. The isotopic shifts in the CO_2 asymmetric stretch region show an interesting pattern. While in the C−O stretch region the shifts of the ^{13}C and ^{18}O isotopes are comparable and take place as per the simple isotopic shift rule, in the CO_2 region the ^{18}O shift is much less than the ^{13}C shift (Table 2, Figure 14). This can be accounted for by the formation of only isotopically asymmetric CO_2, i.e., $^{16}OC^{18}O$, and not of a symmetric species, i.e., $^{18}OC^{18}O$. This is so, since for the symmetric molecule, the ν_3 mode is the only mode in the $\sum_u^+$ species of the $D_{\infty h}$ point group, and the entire isotope shift on substitution of ^{18}O comes in this mode, while for the isotopically asymmetric molecule both the C−O stretching modes belong to $\sum^+$ of the $C_{\infty v}$ group, and the isotope shift is shared between them. The calculated isotope shifted frequency for say the 2351 cm^{-1} band in the symmetric substituted case will be 2283 cm^{-1}, which is much larger than the observed shift. For the asymmetrically substituted molecule, if we assume that the total shift is shared between the two stretching modes,[33] both of which belong to the same symmetry species now, the calculated value will be ≈2317 cm^{-1}, which matches the observed value. The isotope shifts in Figure 14 and Table 2 thus lead to the conclusion that the CO interaction with the zeolite gives rise to the formation of only asymmetric $^{16}O-C^{18}O$ molecules.

The possible sources of oxygen may be identified with the reaction of CO with the occluded water molecules, acidic hydroxyl groups, or the structural oxygen ions. Data in Figure 7 show that the yield of CO_2 increased when a zeolite sample was pretreated in situ under vaccum for longer periods (Figure 7b,c). Also, no rotational bands due to water molecules are seen in this figure, thus ruling out a possibility of the CO + H_2O reaction as a possible source of CO_2. The absorbance values given in Figure 15c,d show that the frequency and the intensity of the O−D bands did not change substantially on CO adsorption in the temperature range 300−575 K. It is thus likely that the oxygen ions of zeolitic framework rather than the hydroxyl groups are responsible for the oxidation of CO molecules. An alternative route to CO_2 formation, as pointed out by a referee, could be a rearrangement in CO clusters in zeolitic cavities or the disproportionation of CO molecules at metal impurity sites. However, we do not see even a trace of symmetrically ^{18}O-substituted CO_2 in the spectra of Figure 14c, as will then be expected for $C^{18}O$ adsorption. At the same time, we are now in no position to comment about the mechanistic routes involved in the oxidation of CO vide lattice oxygen. We may though mention that the cleavage of Si−O−Si and Si−O−Al bonds in zeolites and the exchange of oxygen isotopes between the zeolitic framework and the oxygen-containing molecules have been demonstrated by various workers.[34,35]

The asymmetric ν_3 bands of CO_2 show almost similar behavior as that of CO in terms of the isotopic shifts and the

dependence of their intensity on the adsorbate pressure and on the nature of the charge-balancing cation (Figures 6, 7, and 11). For instance, all the bands, namely 2336, 2348, 2356, and 2364 cm^{-1} bands, exhibit an identical shift in frequency on cation exchange (Figure 6) and also when the isotopically labeled ^{13}CO was used as adsorbate (Figure 14, Table 2). The effect of pressure on the growth of $\nu_3(CO_2)$ bands (Figure 11) also followed a behavior similar to that of CO (Figures 8 and 9).

In analogy with the arguments given above in favor of the existence of $(CO)_n$ clusters, we may thus attribute the ν_3 region bands of CO_2 (Figure 6) to the molecular ensembles of carbon dioxide, even though the bonding involved in these clusters is not clear at present.

References and Notes

(1) Angell, C. L.; Schaffer, P. C. *J. Phys. Chem.* **1966**, *70*, 1413.

(2) Rabo, J. A.; Angell, C. L.; Kasai, P. H.; Schomaker, V. *Discuss. Faraday Soc.* **1966**, *41*, 328.

(3) Egerton, T. A.; Stone, F. S. *J. Chem. Soc., Faraday Trans. 1* **1973**, *69*, 22.

(4) Zecchina, A.; Bordiga, S.; Spoto, G.; Scarano, D.; Petrini, G.; Leofanti, G.; Padovan, M.; Arean, G. O. *J. Chem. Soc., Faraday Trans. 1* **1992**, *88*, 2959.

(5) Bordiga, S.; Platero, E. F.; Arean, C. O.; Lamherti, C.; Zecchina, A. *J. Catal.* **1992**, *137*, 179.

(6) Bordiga, S.; Searano, D.; Spoto, G.; Zecchina, A. *Vib. Spectrosc.* **1993**, *5*, 69.

(7) Gruver, V.; Fripiat, J. J. *J. Phys. Chem.* **1994**, *98*, 8549.

(8) Chem, L.; Lin, L.; Xu, Z.; Zhang, T.; Xim, Q.; Ying, P.; Li, G.; Li, C. *J. Catal.* **1996**, *161*, 107.

(9) Palomino, G. T.; Arean, C. O.; Geobaldo, F.; Ricchiardi, G.; Bordiga, S.; Zecchina, A. *J. Chem. Soc., Faraday Trans. 1* **1997**, *93*, 189.

(10) Knozinger, H. In *Elementary reaction steps in Heterogeneous Catalysis*; Joyner, R. W., Van Santen, R. A., Eds.; Plenum Press: New York, 1994; p 267.

(11) Neyman, K. M.; Strodel, P.; Ruzankin, S. Ph.; Schlensog, N.; Knozinger, H.; Röschm, N. *Catal. Lett.* **1995**, *31*, 273.

(12) Beebe, T. P.; Gelin, P.; Yates, Jr., J. T. *Surf. Sci*. **1984,** *148*, 526.

(13) Kubelkova, L.; Beran, S.; Lercher, J. A. *Zeolites* **1989**, *9*, 539.

(14) Kamble, V. S.; Gupta, N. M.; Kartha, V. B.; Iyer, R. M. *J. Chem. Soc., Faraday Trans. 1* **1993**, *89*, 1143.

(15) Kamble, V. S.; Gupta, N. M.; Iyer, R. M. *J. Catal.* **1988**, *113*, 398.

(16) Gupta, N. M.; Kamble, V. S.; Annaji Rao, K.; Iyer, R. M. *J. Catal.* **1989**, *120*, 432.

(17) Breck, D. W. *Zeolite Molecular Sieves*; John Wiley & Sons: New York, 1974; p 347.

(18) Gupta, N. M.; Kamble, V. S.; Iyer, R. M.; Thampi, K. R.; Gratzel, M. *J. Catal.* **1992**, *137*, 473.

(19) Shete, B. S. Ph.D. Thesis, Mumbai University, 1998.

(20) Gates, B. C.; Katzer, J. R.; Schuit, G. C. A. In *Chemistry of Catalytic Processes*; McGraw-Hill: New York, 1979; p 49.

(21) Zaki M. I.; Knözinger, H. *Spectrochim. Acta* **1987,** *43A*, 1455.

(22) Zecchina, A.; Arean, C. O. *Chem. Soc. Rev.* **1996**, 187**.**

(23) Ballinger, T. H.; Yates Jr., J. T. *Langmuir* **1991**, *7*, 3041.

(24) Zecchina, A.; Platero, E. E.; Arean, C. O. *J. Catal*. **1987**, *107*, 244.

(25) Ward, J. W. In *Zeolite Chemistry and Catalysis;* Rabo, J. A., Ed.; American Chemical Society: Washington, DC, 1976, ACS Monograph 171, p 126.

(26) Hush, N. S.; Williams, M. L. *J. Mol. Spectrosc.* **1974**, *50*, 349.

(27) Haynes, H. W., Jr. *Catal. Rev.—Sci. Eng.* **1978**, *17*, 273.

(28) Rabo, J. A.; Angell, C. L.; Kasai, P. H.; Schomaker, V. In *The Role of the Adsorbed State in Heterogeneous Catalysis*; Discussion of the Faraday Society No. 41; The Faraday Society: London, 1966; p 332.

(29) Rao, L. F.; Fukuoka, A.; Ichikawa, M. *J. Chem. Soc., Chem. Commun.* **1988**, 458.

(30) Shen, L. L.; Knozinger, H.; Sachtler, W. M. H. *Catal. Lett*. **1989**, *2*, 129.

(31) Kawi, S.; Gates, B. C. *J. Chem. Soc., Chem. Commun.* **1992**, 702.

(32) Kawi, S.; Chang, J. R.; Gates, B. C. *J. Catal*. **1993**, *142*, 585.

(33) Herzberg, G. *Infrared and Raman Spectra*; D. Van Nostrand: New York, 1960; p 231.

(34) Jocobs, P. A.; Van Cauwelaert, F. H.; Vansant, E. F.; Uytterhoeven, J. B. *J. Chem. Soc., Faraday Trans. 1* **1973**, *69*, 1056.

(35) Takaishi, T.; Endoh, A. *J. Chem. Soc., Faraday Trans. 1* **1987**, *83*, 411.